Korean J. Chem. Eng., **29**(1), 125-129 (2012)
DOI: 10.1007/s11814-011-0145-y

Synthesis of polypyrrole-reduced graphene oxide composites by in-situ photopolymerization and its application as a supercapacitor electrode

Hai Dinh Pham, Viet Hung Pham, Eun-Suok Oh, Jin Suk Chung, and Sunwook Kim†

School of Chemical Engineering and Bioengineering, University of Ulsan, Ulsan 680-749, Korea
(*Received 17 March 2011 • accepted 29 May 2011*)

Abstract–A highly conductive polypyrrole (PPy)-reduced graphene oxide (RGO) composite with an electrical conductivity of 610 S m^{-1} was successfully synthesized by the in-situ photopolymerization of pyrrole in a graphene oxide suspension. Graphene oxide (GO) played the role of an electron acceptor and was reduced as it accepted electrons. The reduction of GO was confirmed by the increase in the C/O ratio of RGO with the UV irradiation time as well as the high electrical conductivity of PPy-RGO composite. Through the thermogravimetric analysis, it has been found that the PPy-RGO composite exhibited high thermal stability compared to the GO and PPy. This material was used as an electrode in a supercapacitor cell and showed excellent performance for electrical energy storage. The composite exhibited a specific capacitance of 376 F g^{-1} at a scan rate of 25 mV s^{-1}.

Key words: Polypyrrole, Graphene Oxide, Photopolymerization, Supercapacitor, Electrode

INTRODUCTION

Graphene, a flat monolayer of carbon atoms packed into a two-dimensional honeycomb lattice, has attracted a great deal of scientific interest due to its excellent electronic, mechanical, thermal properties and its high surface area [1]. Chemically modified graphene (CMG) produced from graphite and its derivatives is considered to be a promising nanofiller for polymer composites [2,3]. The incorporation of CMG into a polymer matrix has resulted in a significant improvement in the properties of the host material [4-8]. Polypyrrole (PPy) is one of the most promising electrically conducting polymers (ECPs) for multifunctional applications such as electrodes for batteries and supercapacitors, sensors, electrochromic windows, anti-electrostatic coatings and functional membranes [9]. The incorporation of polypyrrole with carbon materials has been shown to enhance the specific capacitance and electochemical behavior of the supercapacitor electrode. The maximum specific capacitance of 265 F g^{-1} has been obtained by incorporating PPy into SWNT [10]. Biswas and Drzal [11] developed a multilayer composite electrode by combining nanostructured polypyrrole and graphene nanosheets resulting in a specific capacitance of 165 F g^{-1} and low electronic resistance for supercapacitor electrode applications.

However, because of their high specific area, graphene sheets tend to form irreversible agglomerates or even restack due to van der Waals interactions [12]. Such issues must be resolved when preparing graphene-based nanocomposites. At present, the most popular strategy to prepare CMG-based polymer composites is to disperse the polymer [4,6] or to perform in-situ polymerization [7,8] in a graphene oxide (GO) suspension, where GO is subsequently reduced to graphene with hydrazine or a derivative of hydrazine. In preparing CMG/polymer composite using those processes, the decrease of the GO reduction efficiency due to the presence of a polymer and the contamination of a composite by the reducing agent are inevitable.

The photopolymerization of pyrrole is an interesting approach to synthesize PPy [14] and its composites with metal nanoparticles [15,16] or semiconducting metal oxides [12,17]. The photopolymerization process has been carried out by exposing a mixture of pyrrole monomers and electron acceptors (such as group 1B metal ions) or photoactive species (such as semiconducting metal oxides) to UV light. Incorporating metal and metal oxide cluster into ECPs is known to enhance their conductivity and catalytic property [17]. The pyrrole monomers absorb photons and form photoexcited pyrrole molecules that are immediately quenched by the electron acceptor in the formation of pyrrole radical cations. It is these radicals that initiate the photopolymerization of pyrrole [14,15,17].

PPy is one of the most important conducting polymers for supercapacitor applications [9] and graphene is emerging as an excellent electrode material [18]. Therefore, PPy-reduced graphene oxide (PPy-RGO) composites have the potential to be the active material in supercapacitor electrodes. In this work, we focus on the synergistic effects from the interaction of pyrrole, PPy and GO by in-situ photopolymerization. Graphene oxide and pyrrole formed electron donnor/acceptor pair and highly conductive PPy-RGO composites could be succesfully synthesized by using long wave ultraviolet (UVA) irradiation. In the in-situ photopolymerization, GO played the role of an electron acceptor and was reduced as it accepted electrons.

EXPERIMENTAL

1. Chemicals

Expandable graphite (Grade 1721) was supplied by Asbury Carbon. Concentrated sulfuric acid (H_2SO_4), potassium permanganate ($KMnO_4$), hydrochloric acid (HCl), hydrogen peroxide (H_2O_2) and pyrrole monomer (Pyrrole 98%) were purchased from Aldrich. All

†To whom correspondence should be addressed.
E-mail: swkim@ulsan.ac.kr

chemicals were used as received without further purification.

2. Synthesis of GO

A small amount of expandable graphite was charged into a 1-L beaker and heated for 10 s in a microwave oven (Panasonic, NN-5653A). The graphite expanded to about 150 times its original volume. Graphene oxide (GO) was synthesized from expanded graphite according to a modified Hummer method [19]. Typically, 500 mL of concentrated H_2SO_4 was charged into a 3-L, three-necked flask equipped with a mechanical stirrer (Teflon impeller). The flask was put into an ice bath to chill down to 0 °C. Five grams of expanded graphite were gradually added under stirring to make a suspension. Then, 30 g of $KMnO_4$ was slowly added so that the temperature did not exceed 20 °C. The temperature was then elevated to 35 °C, and the suspension was stirred for 2 h. The flask was chilled again in the ice bath, and 1 L of deionized water was slowly added to maintain a temperature below 70 °C. The mixture was stirred for 1 h and subsequently diluted with 5 L of deionized water. Fifty milliliters of H_2O_2 (30 wt%) was slowly added, and vigorous bubbles appeared as the suspension changed from dark brown to yellow. The suspension was centrifuged and washed with 10% HCl solution four times followed by centrifuging at 10,000 rpm. And the solid was washed with deionized water to completely remove the acid until the pH of the GO dispersion reached 6. The as-synthesized GO dispersion was a paste. The concentration of GO was 1.0 wt%, which was determined after drying the GO dispersion at 80 °C under vacuum for 24 h.

3. Photopolymerization

In a typical photopolymerization, 1 mL of pyrrole was added to a 200 mL GO suspension (0.1 mg mL^{-1}) under stirring. Upon the addition of pyrrole to the GO suspension, some particles that were visible with the naked eye slowly appeared. The appearance of such particles indicated a change in the hydrophilicity of the GO due to the adsorption of pyrrole on the surface of GO sheets through π-π stacking. The pyrrole-GO suspension was then exposed to UVA irradiation (365 nm, 80 W). The color of the pyrrole-GO suspension gradually changed from brown to dark green and then to black after 4 h. After 24 h, the resultant slurry was filtered and rinsed with water and acetone so as to remove unreacted pyrrole and oligomers. The washed slurry was ultimately dried at 80 °C.

4. Characterization

The UV-vis absorbance of GO and PPy-RGO in ethanol as functions of reduction time were measured by a microplate spectrophotometer (Spectra Max® Plus 384). The elemental compositions of GO and PPy-RGO composite were analyzed by an element analyzer (Flash 2000, Thermo Scientific). The thermogravimetric analysis (TGA) of GO and PPy-RGO was characterized under nitrogen atmosphere at a heating rate of 10 °C min^{-1} (Q50, TA Instrument). The atomic force microscope (AFM) image was taken using a Veeco dimension 3100 SPM with a silicon cantilever operated in the tapping mode. The electrical resistance of CCG-P paper was measured by the four-point probe method using Advanced Instrument Technology (AIT) CMT-100 MP with a Jandel Engineering probe.

5. Electrochemical Measurements

The electrochemical properties and capacitance measurements of supercapacitor electrodes were studies in two-electrode system by cyclic voltammetry (CV) and electrochemical impedance spectroscopy (EIS) using IVIUMSTAT instrument (IVIUM Technologies, Netherlands). The specific capacitance value was obtained from the CV curves according to the equation:

$$c = 4\frac{I}{\left(m\frac{dV}{dt}\right)}$$

where I is the current during discharge (from V_{max} to zero volts) and m is the weight of active material in electrode [19].

Electrode was fabricated by mixing 5 mg of PPy-RGO with 1.6 mg carbon black and 1.6 mg poly(vinylidene fluoride) (PVDF) in NMP (10% PVDF w/w). Mixture was ground in mortar and then pressed into 1 cm^2 pellets. The two electrodes were separated by a glass fiber membrane in 1 M H_2SO_4 aqueous electrolyte solution. Electrodes were dried for 1 hour at 120 °C to make solvent evaporate. Impedance spectroscopy was carried out at bias 0.1 V with sinusoidal signal of 5 mV over the frequency range from 100 kHz to 1 MHz.

RESULTS AND DISCUSSION

The photopolymerization of the pyrrole was monitored by UV-vis spectroscopy. As shown in Fig. 1(a), pyrrole exhibited a very

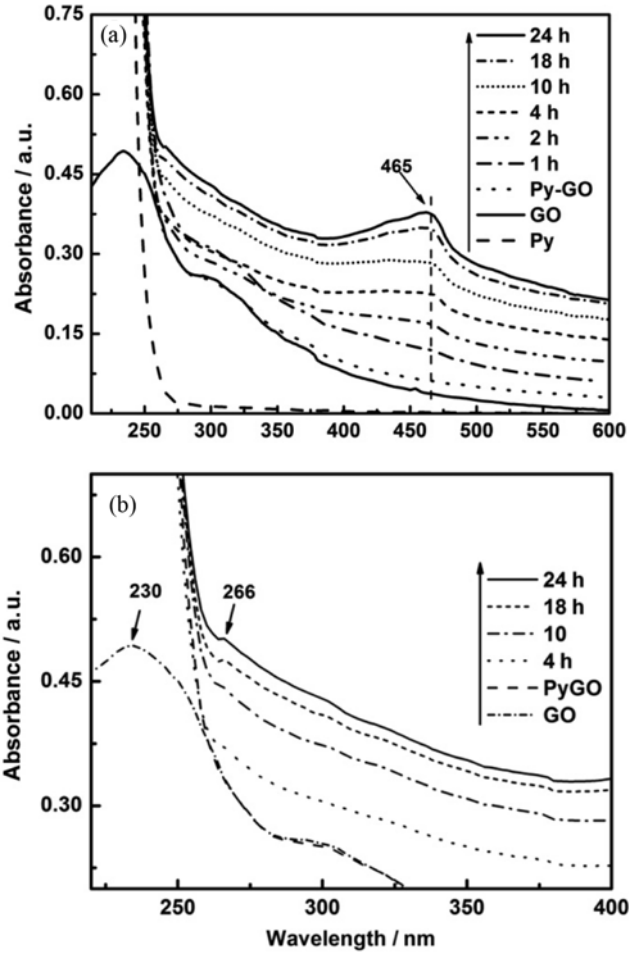

Fig. 1. The change in the UV-vis absorption spectra of PPy-RGO composites by varying the UV irradiation time (a), enlarged UV-vis absorption spectra between 200 and 400 nm (b).

strong absorption peak at 200-240 nm; there was no absorbance in the higher wavelength region. The GO exhibited a main absorption peak centered at 234 nm and a shoulder at 300 nm. The spectrum of the Py-GO mixture exhibited Py absorption characteristics at wavelengths up to 250 nm, and then showed GO absorption behavior of a higher intensity in the remaining spectral region. The latter behavior was the result of an interaction between the Py and GO. After UV irradiation for 1 h, no absorption peaks appeared but the absorption intensity in the entire spectral region increased significantly, especially in the range of 260-350 nm. Such an increase was caused by the absorption of terpyrrole (305 nm) and quarterpyrrole (340 nm) oligomers [17]. After 4 h, the absorption peak at 465 nm corresponding to the π-π^* transition of PPy [16,17] clearly appeared and indicated the formation of PPy. It should be noted that the UV light used in this work was located at 365 nm and does not have enough energy to photoexcite Py and to reduce GO. Therefore, it could be assumed that the π-π^* interaction between the Py and GO lowered the photoexciation energy of the Py. The intensity of both the absorption in the entire spectral region and the π-π^* transition peak gradually increased with the UV irradiation. After 20 h, little increase in the absorption intensity was observed, which suggested the completion of the photopolymerization process. According to the results by Li and co-workers [12], the formation of RGO by using hydrazine as a reducing agent was detected by the red-shift of absorption peaks from 234 nm to 265 nm. The enlarged portion of the UV spectra from 200 nm to 400 nm is illustrated in Fig. 1(b) to clearly show the red-shift of absorption peaks. After 4 h (especially at 24 h), the red-shifted absorption peak due to the formation of RGO appeared at 266 nm. And the absorption peak of GO at 300 nm disappeared.

The elemental analysis results in Table 1 showed that the nitrogen content increased with the UV irradiation time. This finding was consistent with an increase in the mass ratio of PPy/RGO from 0.56 to 1.38 when the irradiation time was increased from 4 to 24 h. Composition of RGO was calculated by subtracting carbon from PPy in PPy-RGO. The elemental composition analysis also revealed that the C/O atomic ratio of RGO increased from 1.68 (GO) to 2.26 and 3.10 after 4 and 24 h UV irradiation, respectively. The increase in the C/O ratio of RGO with the UV irradiation time demonstrates that some of the oxygen functional groups were removed during the photopolymerization.

To further confirm the reduction of the GO, PPy/RGO composites were compressed into pellets at 4,000 psi and their electrical conductivities were measured with the four-point probe technique. These conductivity values were then compared with the electrical conductivity of PPy synthesized with ammonium persulfate without GO and HCl. As listed in Table 2, PPy exhibited a very low electrical conductivity (1.2×10^{-2} S m^{-1}), whereas PPy-RGO showed a conductivity that was 4-5 orders of magnitude higher than that of PPy. In addition, PPy-RGO exhibited 2 orders of magnitude higher electrical conductivities than those of photopolymerized PPy-Au composites [13]. The electrical conductivity of PPy-RGO-24h was significantly higher than that of PPy-RGO-4h, although the increase in the electrical conductivity was not proportional to an increase in the PPy/RGO ratio.

Table 2. Electrical conductivities of PPy and PPy-RGO composites

Sample	PPy	PPy-RGO-4 h	PPy-RGO-24 h
Electrical conductivity (S m^{-1})	0.012	345	610

The morphology of the PPy-RGO composites was examined via scanning electron microscopy (SEM) and atomic force microscopy (AFM). As seen in the SEM image, the surface of PPy-RGO was rough and corvered by PPy. And most of the PPy was located on both sides of the GO sheets, while only a small fraction of the PPy existed as granular agglomerates. The thickness of a PPy-RGO sheet (as determined from AFM images) was around 5.5 nm, which is about 5 times thicker than the GO sheet (1.1 nm). From the AFM image of PPy-RGO in Fig. 2, it is believed that the portion of PPy-RGO particle to show surface profile does not contain overlapped particles. Therefore, the enhanced thickness of a PPy-RGO sheet (5.5 nm) was thought to result from the presence of PPy on the surface of RGO. However, to confirm the structure of the PPy-RGO particle precisely, it would be beneficial to perform HRTEM analysis in addition to the AFM measurement, which will be done in the future communication. Another discussion on the enhanced thickness of PPy-RGO can be made based on the mechanism of the photopolymerization process. From the UV-vis result, it has been said that pyrrole was firstly adsorbed on GO sheet and the π-π^* interaction between the Py and GO lowered the photoexciation energy of the Py. Electron produced from nucleations was directly transferred to GO and reduced GO to RGO. Propagation process of photopolymerization could be happened when pyrrole interacted to surface of PPy-RGO. Such a scenario indicates that the nucleation and propagation processes of photopolymerization occurred on the surface of the GO sheets. This could be clear evidence that GO plays the role of an electron acceptor.

The thermal properties of the PPy-RGO composites were characterized by thermo gravimetric analysis (TGA) in a nitrogen atmo-

Table 1. Elemental composition of GO, PPy, and PPy-RGO composites

Sample	C (wt%)	O (wt%)	N (wt%)	H (wt%)	C/O ratio	PPy/RGO
GO	54.53	43.29	-	2.18	1.68	-
PPy	73.85	-	21.54	4.61	-	-
PPy-RGO 4 h	65.71	23.08	7.88	3.53	-	0.56
PPy-RGO 24 h	71.38	12.28	12.53	3.81	-	1.38
RGO 4 h*	61.25	36.14	-	2.61	2.26	-
RGO 24 h*	68.02	29.26	-	2.72	3.10	-

*Elemental composition of RGO was calculated from the PPy-RGO composition

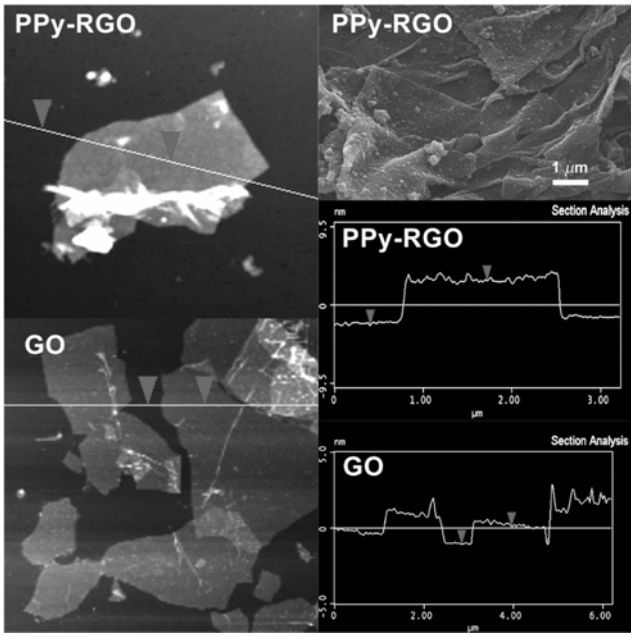

Fig. 2. SEM/ AFM images of GO and PPY-RGO composite.

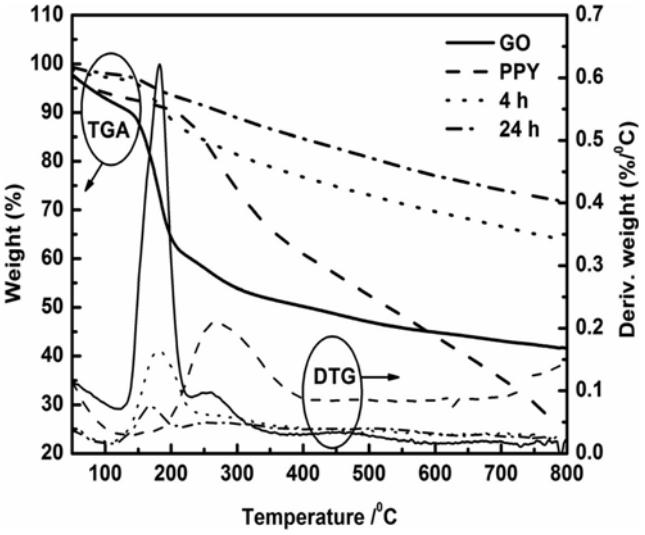

Fig. 3. TGA results of PPy, GO, and PPy-RGO composites.

sphere with a heating rate of 10 °C min^{-1}. These thermal characteristics of the composites were then compared with those of GO and PPy, as shown in Fig. 3. The GO lost about 55% of its weight when the temperature reached 800 °C. The derivative of the thermogravimetric (DTG) curve for GO showed sharp peaks around 175 and 250 °C that correspond to the decomposition of labile oxygen functional groups and carboxylic groups, respectively [18]. In the case of PPy, an approximately 75% loss in weight occurred at 800 °C with a sharp DTG peak at 270 °C. In contrast, the PPy-RGO composites exhibited high thermal stability when compared to the GO and PPy. The weight losses of the PPy-RGO-4h and PPy-RGO-24h were 36% and

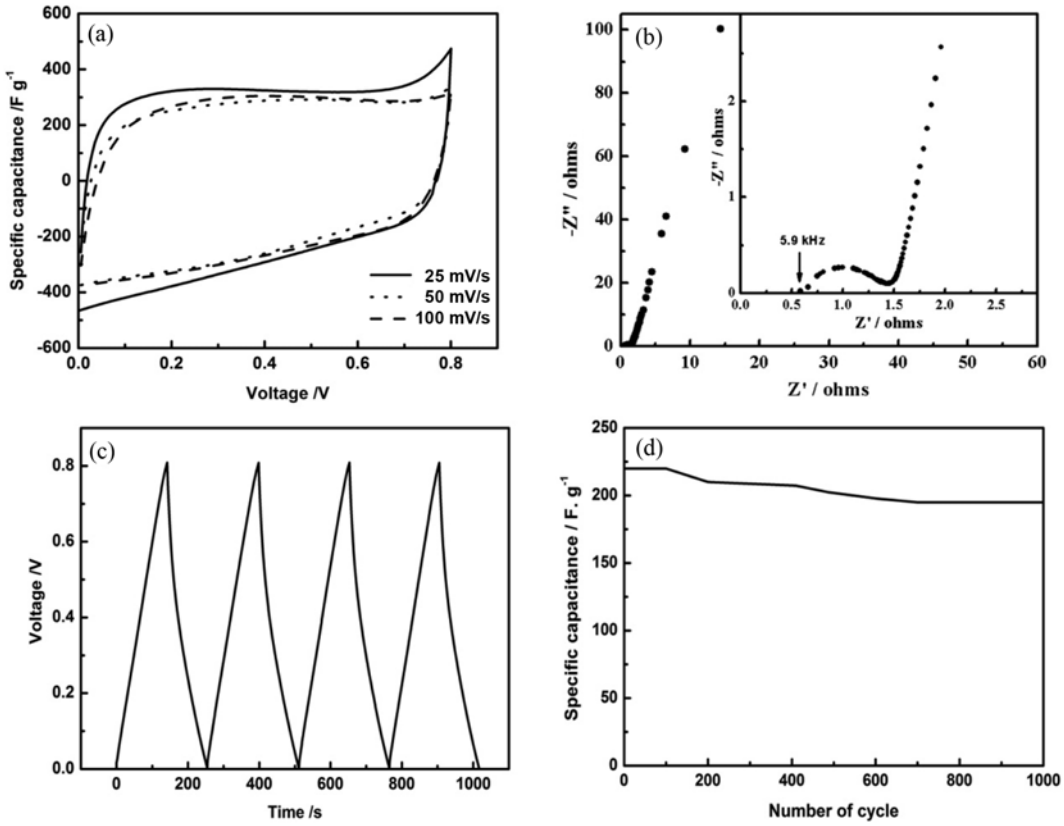

Fig. 4. Cyclic voltammogram of PPy-RGO composite (a), Nyquist plot of PPy-RGO composite (b), charge/discharge test with applied current density of 200 mAg^{-1} in the potential range between 0 and 0.8 V (c), cycle stability of PPy-RGO at current density of 1 A g^{-1} (d).

28% at 800 °C, respectively. DTG curves revealed that the main decomposition peaks of the PPy-RGO composites were located around 175 °C and their intensities were much smaller than that of GO. The decrease in the intensity of the decomposition peak at 175 °C may be due to the removal of labile oxygen functional groups during the photopolymerization process. The DTG curves from the PPy-RGO composites showed that the decomposition rates in the temperature range of 250-800 °C were significantly lower than that those of PPy. Thus, it can be concluded that the thermal properties of PPy are effectively improved by the incorporation of PPy into RGO.

To evaluate the potential for practical electrical energy storage, PPy-RGO composite was used as an electrode material. A two-electrode test cell with a 1 M H_2SO_4 electrolyte was used to characterize the electrochemical properties of PPy-RGO via cyclic voltammetry (CV), charge - discharge test and electrochemical impedance spectroscopy (EIS). As shown in Fig. 4(a), the specific capacitance calculated from the CV data at a scan rate of 25 mV s^{-1} was 376 F g^{-1}, which is significantly higher than that attained with MWNT-PPy (192 F g^{-1}) [21] or graphene-PPy (169 F g^{-1}) [11] composites. Even at a high scan rate of 100 mV s^{-1}, the specific capacitance reached 275 F g^{-1}. The CV curves shown in Fig. 4(a) are nearly rectangular and the specific capacitance slightly decreased with an increase in the scan rate voltage from 25 to 100 mV s^{-1}. Such behavior indicated good charge propagation within the electrodes. The Nyquist plot in Fig. 4(b) exhibited good capacitor-like behavior with small diffusion limitations. In the high frequency intercept of real axis, the high conductivity of PPy-RGO contributed to the low equivalent series resistance (ESR) of the cell [22,23]. The internal cell resistance was 0.58 Ω at 5.9 kHz (real Z' axis). In the low frequency region, the short Warburg region in the Nyquist plot indicates a low diffusion resistance for ions in the electrodes [22]. Fig. 4(c) shows a constant current charge/discharge test of the PPy-RGO electrode with the current density of 200 mA g^{-1} in the potential range between 0 and 0.8 V. The charge/discharge curves showed nearly ideal straight line, indicating pseudocapacitance behavior. As illustrated in Fig. 4(d), the cycle stability of PPy-RGO electrode was excellent to show approximately 16% loss of the initial specific capacitance during a thousand cycles at the current density of 1 A g^{-1}.

CONCLUSIONS

Polypyrrole (PPy)-reduced graphene oxide (RGO) composites were successfully synthesized by the in-situ photopolymerization of pyrrole in the presence of graphene oxide (GO). Electrons produced via photopolymerization of pyrrole were transferred to graphene sheet and reduced as it accepted electrons. Even though PPy exhibited a very low electrical conductivity (1.2×10^{-2} S m^{-1}), PPy-RGO-24h showed a conductivity of 610 S m^{-1}, which was 4-5 orders of magnitude higher than that of PPy. PPy-RGO composites exhibited high thermal stability when compared to the GO and PPy. The specific capacitance calculated from the CV data at a scan rate of 25 mV s^{-1} was 376 F g^{-1}, and specific capacitance could remain 84% after a thousand cycles. The composite synthesized by this method showed very good performance for electrical energy storage application.

REFERENCES

1. A. K. Geim and K. S. Novoselov, *Nature Mater.*, **6**, 183 (2007).
2. B. Z. Jang and A. Zhamu, *J. Mater. Sci.*, **43**, 5092 (2008).
3. S. Park and R. S. Ruoff, *Nature Nanotechnol.*, **4**, 217 (2009).
4. S. Stankovich, D. A. Dikin, G. H. B. Dommett, K. M. Kohlhaas, E. J. Zimney, E. A. Stach, R. D. Piner, S. B. T. Nguyen and R. S. Ruoff, *Nature*, **442**, 282 (2006).
5. T. Ramanathan, A. A. Abdala, S. Stankovich, D. A. Dikin, M. Herrera-Alonso, R. D. Piner, D. H. Adamson, H. C. Schiepp, X. Chen, R. S. Ruoff, S. T. Nguyen, I. A. Aksay, R. K. Prud'homme and L. C. Brison, *Nature Nanotechnol.*, **3**, 327 (2008).
6. X. Zhao, Q. Zhang, D. Chen and P. Lu, *Macromolecules*, **43**, 2357 (2010).
7. K. Zhang, L. L. Zhang, X. S. Zhao and J. Wu, *Chem. Mater.*, **22**, 1392 (2010).
8. J. Yan, T. Wei, B. Shao, Z. Fan, W. Qian, M. Zhang and F. Wei, *Carbon*, **48**, 487 (2010).
9. L. X. Wang, X. G. Li and Y. L. Yang, *React. Funct. Polym.*, **47**, 125 (2001).
10. K. H. An, K. K. Jeon, J. K. Heo, S. C. Lim, D. J. Bae and Y. H. Lee, *J. Electrochem. Soc.*, **149**, 1058 (2002).
11. S. Biswas and L. T. Drzal, *Chem. Mater.*, **22**, 5667 (2010).
12. D. Li, M. B. Müller, S. Gilje, R. B. Kaner and G. G. Wallace, *Nature Nanotechnol.*, **3**, 101 (2008).
13. S. Park, J. An, I. Jung, R. D. Piner, S. J. An, X. Li, A. Velamakanni and R. S. Ruoff, *Nano Lett.*, **9**, 1593 (2009).
14. I. Rodriguez and J. Gonzalez-Velasco, *J. Chem. Soc. Chem. Commun.*, **5**, 387 (1990).
15. M. A. Breimer, G. Yevgeny, S. Sy and O. A. Sadik, *Nano Lett.*, **1**, 305 (2001).
16. C. R. Martins, Y. M. De Almeida, G. C. Do Nascimento and W. M. De Azevedo, *J. Mater. Sci.*, **41**, 7413 (2006).
17. Z. Weng and X. Ni, *J. Appl. Polym. Sci.*, **110**, 109 (2008).
18. L. L. Zhang, R. Zhou and X. S. Zhao, *J. Mater. Chem.*, **20**, 5983 (2010).
19. V. H. Pham, T. V. Cuong, T.-D. Nguyen-Phan, H. D. Pham, E. J. Kim, S. H. Hur, E. W. Shin, S. Kim and J. S. Chung, *Chem. Commun.*, **46**, 4375 (2010).
20. M. D. Stoller and R. S. Ruoff, *Energy Environ. Sci.*, **3**, 1294 (2010).
21. M. Hughes, G. Z. Chen, M. S. P. Shaffer, D. J. Fray and A. H. Windle, *Chem. Mater.*, **14**, 1610 (2002).
22. M. D. Stoller, S. Park, Y. Zhu, J. An and R. S. Ruoff, *Nano Lett.*, **8**, 3498 (2008).
23. J. Yan, T. Wei, B. Shao, F. Ma, Z. Fan, M. Zhang, C. Zheng, Y. Shang, W. Qian and F. Wei, *Carbon*, **48**, 1731 (2010).